

Relating the Microwave Backscattering Coefficient to Leaf Area Index

F. T. ULABY, C. T. ALLEN, and G. EGER III*

Remote Sensing Laboratory, University of Kansas Center for Research, Inc., Lawrence, Kansas 66045

E. KANEMASU

Evapotranspiration Laboratory, Kansas State University, Manhattan, Kansas 66506

This paper examines the relationship between the microwave backscattering coefficient of a vegetation canopy, σ_{can}^0 and the canopy's leaf area index (LAI). The relationship is established through the development of one model for corn and sorghum and another for wheat. Both models are extensions of the cloud model of Attema and Ulaby (1978). Analysis of experimental data measured at 8.6, 13.0, 17.0, and 35.6 GHz indicates that most of the temporal variations of σ_{can}^0 can be accounted for through variations in green LAI alone, if the latter is greater than 0.5.

Introduction

Among the prime objectives of agricultural remote sensing is the early and accurate estimation of agricultural production in a manner superior to that of more conventional means. The first step in that direction is the identification of crop types, which usually is accomplished by means of multivariate observations of the particular test site or area of interest. Once the identities of the various field covers in a given area have been determined, crop acreage can be estimated. In order to estimate crop production reliably, an estimate of yield is needed for each of the crop types of fields concerned. In the next section, traditional as well as remote-sensing approaches to crop yield estimation are discussed.

Several papers have been published over the past few years documenting the

ability of radar to identify crop types correctly, i.e., with a classification accuracy of 90% or higher, based on two or three multivariate observations (Bush and Ulaby, 1978; Li et al., 1980; Hoogeboom et al., 1982; Brisco and Protz, 1981; Shanmugan et al., 1983). The purpose of this paper is to examine the relationship between the microwave backscattering coefficient of a vegetation canopy (σ_{can}^0) and the canopy's leaf area index (LAI)—the latter determining the solar radiation intercepted by the canopy, which in turn is an important component of crop-yield models. The means of such an examination is based on an analysis of experimental data in terms of a modified form of the canopy "cloud" model of Attema and Ulaby (1978).

Crop Yield and LAI

The yield of a particular crop is a function of many variables, including the nutrients available to it and the weather

*Mr. Eger is now with Shell Information Services, Houston, Texas.

conditions affecting it over the growing season. Successfully estimating a crop's yield requires knowledge of factors that include the health of the plants and their vigor at various points in time, the amount of fertilizer and water available to them, and hourly or daily weather-condition information (Daughtry and Fuhs, 1980). Meteorological information is available from organizations such as NOAA for the United States and related regions, and from the World Meteorological Organization (WMO) for worldwide weather monitoring.

Early attempts to predict yields were based upon such factors as previous years' yield, improvements in technology, and the effects of current weather conditions (MacDonald and Hall, 1980). By incorporating *a priori* knowledge such as soil type and water-table level, estimates of soil moisture information are added to the model, thus improving its predictive capacity. The amount of available solar radiation, which is the basic source of energy in the process of photosynthesis, is also a major determinant of overall yield.

As an energy source, solar radiation is available to the plant only when it interacts with the leaves. Thus, an estimate of the total area of exposed and active leaves, in conjunction with incident solar radiation, provides another measure of crop performance, and consequently of final yield. This was the reasoning used by Dale (1977) in the development of the energy-crop-growth (ECG) model. This model takes the form

$$\text{ECG} = \sum_{i=t_1}^{t_2} (\text{SR}/600)_i \times (\text{SRI})_i (\text{WF})_i (\text{FT})_i, \quad (1)$$

where SR is the daily solar radiation, WF is the ratio of daily evapotranspiration to potential evapotranspiration (Stuff and Dale, 1978), and FT is a daily temperature function that relates growth rate to temperature (Coelho and Dale, 1980). The term "solar radiation intercepted" (SRI) refers to the component that relates the available energy to that interacting with the leaves (Linville et al., 1978).

For the maize (corn) canopy, Linville et al. (1978) have related SRI to leaf area index (L) using the following equation:

$$\text{SRI} = 1 - \exp(-0.79 \cdot L), \quad (2)$$

which has a range from zero to one and reaches 90% when L is about 2.9, as shown in Fig. 1.

Investigators working in the optical region of the electromagnetic spectrum have related the ratio of an IR-band radiance and a red-band radiance to LAI to monitor plant performance for corn and wheat (Daughtry and Fuhs, 1980; Tucker et al., 1981). They have found that, by integrating this ratio over a given period of time, accumulated dry matter may be estimated. In the report by Daughtry et al. (1983), a coefficient of determination $r^2 = 0.7$ was obtained between the true yield

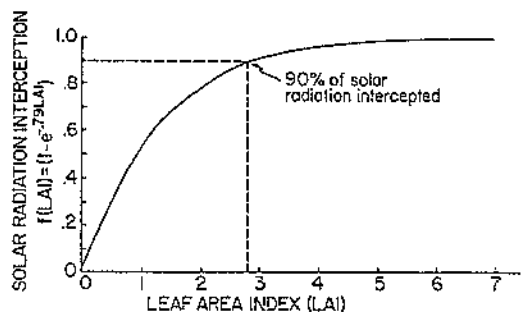


FIGURE 1. Solar radiation weighting factor for determining interception of solar energy by crop as a function of its leaf-area index (from Daughtry et al., 1982).

of corn and the yield estimated from spectral and meteorological data.

Vegetation Canopy Model

In the microwave region, a vegetation canopy may be modeled as a lossy volume of scattering elements, bounded by air above and by a scattering soil surface below [Fig. 2(a)]. The backscattering coefficient σ_{can}^0 represents the sum of the contributions from the canopy itself, from direct backscattering by the soil (including two-way attenuation to account for propagation between the air-canopy boundary and the canopy-soil boundary and back), and from multiple scattering between the canopy scattering elements and the soil surface.

In general, the scattering behavior of the canopy volume is governed by the dielectric properties and geometric configurations of the scattering elements (leaves, stalks, and fruit), the latter being

defined with respect to the wavelength, direction, and polarization of the incident wave. A first-order canopy backscattering model was developed by Attema and Ulaby (1978), who treated the canopy as a water cloud consisting of a collection of identical water particles [Fig. 2(b)] characterized by a uniform scattering phase function. The water-cloud assumption is a consequence of the domination of the dielectric constant of green vegetation (which is a mixture of vegetative matter and water) by the dielectric constant of water. The relative dielectric constant of water is about 80 (below 10 GHz), and the dielectric constant of dry vegetation is on the order of 2–3 (Carlson, 1967; Jedlicka and Ulaby, 1983). Ignoring second-order contributions resulting from multiple scattering between the canopy particles and the soil surface, the backscattering coefficient of the canopy (including soil contributions) is given by

$$\sigma_{\text{can}}^0(\theta) = \sigma_{\text{veg}}^0(\theta) + \sigma_s^0(\theta), \quad (3)$$

where σ_{veg}^0 is the contribution of the vegetation volume, σ_s^0 is the backscattering contribution of the soil surface in the presence of vegetation cover, and θ is the angle of incidence relative to nadir. Assuming the scattering water particles to be uniformly distributed within the canopy volume, Attema and Ulaby (1978) derived an expression for $\sigma_{\text{veg}}^0(\theta)$ by integrating the backscattering contributions of thin strata between the air-vegetation boundary and the vegetation-soil boundary,

$$\sigma_{\text{veg}}^0(\theta) = \frac{\sigma_v \cos \theta}{2\kappa_e} [1 - \Upsilon^2(\theta)], \quad (4)$$

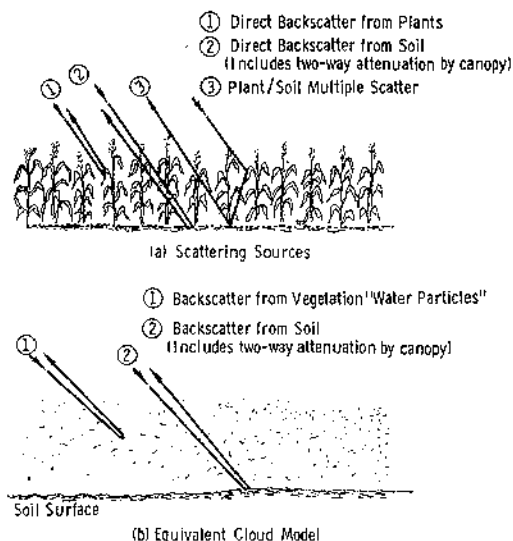


FIGURE 2. Backscattering contributions from a vegetation canopy, (a) scattering sources, and (b) equivalent "cloud" representation in terms of water scatterers.

where

$$\begin{aligned} \Upsilon^2(\theta) &= \exp(-2\kappa_e h \sec \theta), \\ h &= \text{canopy height (m)}, \\ \kappa_e &= \text{canopy extinction} \\ &\quad \text{coefficient (m}^{-1}\text{)}, \\ \sigma_v &= \text{canopy volume back-} \\ &\quad \text{scattering coefficient} \\ &\quad \text{(m}^{-1}\text{)}, \text{ and } \Upsilon^2 \text{ is the two-} \\ &\quad \text{way transmittance of the} \\ &\quad \text{canopy (m}^2 \cdot \text{m}^{-2}\text{)}. \end{aligned} \quad (5)$$

The soil backscattering coefficient, $\sigma_s^0(\theta)$, depends on the soil's surface roughness and its dielectric properties, the latter being governed strongly by the moisture content of the soil surface layer. When radar is used as a vegetation monitor, the angle of incidence θ usually is chosen to be greater than 40° and the wavelength is chosen to be on the order of 3 cm or shorter. Both choices are made, in part, in order to make Υ as small as possible, thereby decreasing the soil backscattering contribution [the second term in (3)] to a negligible level in comparison to the vegetation backscattering contribution. If the second term in (3) is indeed much smaller than the first, it may be neglected. In general, however, σ_s^0 may be described by the simple expression (Attema and Ulaby, 1978)

$$\sigma_s^0(\theta) = [C_s(\theta)m_s] \Upsilon^2(\theta), \quad (6)$$

where $C_s(\theta)$ is a constant for a given wavelength and polarization configuration and m_s is the soil moisture content. The above expression is valid for $m_s \geq 0.05 \text{ g} \cdot \text{cm}^{-3}$. In general, $C_s(\theta)$ is a function of the soil surface roughness, but if

$\lambda \leq 3 \text{ cm}$, $C_s(\theta)$ is approximately roughness-independent over the range of random roughness usually encountered in the case of agricultural crops.

Cloud Model in Terms of Canopy Water Content

Attema and Ulaby (1978) assumed that the "equivalent" scattering water particles of the vegetation volume are all spherical in shape, identical in size, and small relative to the wavelength λ , in which case,

$$\sigma_v = N\sigma_b, \quad (7)$$

$$\kappa_e = NQ_e, \quad (8)$$

where $N \text{ (m}^{-3}\text{)}$ is the number of scattering particles per unit volume and $\sigma_b \text{ (m}^2\text{)}$ and $Q_e \text{ (m}^2\text{)}$ are the backscattering cross section and extinction cross section for a single particle, respectively. For an atmospheric water cloud, κ_e is directly proportional to the cloud's volumetric water content $m_v \text{ (kg} \cdot \text{m}^{-3}\text{)}$. Hence, for the canopy "cloud," κ_e may be expressed as

$$\kappa_e = A_1 m_v, \quad (9)$$

where A_1 is considered a constant at a given wavelength λ . In general, A_1 may also be a function of the physical temperature of the canopy (through the temperature dependence of the dielectric constant of water), the wave polarization, and the shapes and sizes of the real scattering elements (leaves, stalks, and fruit). Approaches that incorporate some of the geometrical characteristics of the canopy are discussed in the next section.

Similarly,

$$\sigma_v = A_2 m_v, \quad (10)$$

where A_2 is a constant, and

$$\frac{\sigma_v}{2\kappa_e} = \frac{A_2}{2A_1} \triangleq A_3. \quad (11)$$

Hence, the above ratio, which appears as the front part of the expression given by (4), is a constant. This is a consequence of the assumption that all the equivalent water particles are spherical in shape and identical in size. If the particles are spherical but their sizes are distributed over a range of values, the relation given by (9) will continue to hold, but that given by (10) may not. For an atmospheric cloud, for example, σ_v is proportional to m_v^2 rather than to m_v . Hence, in general, the ratio on the right-hand side of (11) may be written in the form

$$\sigma_v/2\kappa_e = f(N), \quad (12)$$

where $f(N)$ is a function that depends on the number density of particles N , and may depend on the size-, shape-, and orientation-distributions of the particles. A functional form defining $f(N)$ in terms of leaf area index (LAI) is given in a future section.

Upon inserting (4), (6), (9), and (12) into (3) and (5), the following expressions are obtained:

$$\sigma_{\text{can}}^0(\theta) = f(N) \cos \theta [1 - \Upsilon^2(\theta)] + \Upsilon^2(\theta) C_s(\theta) m_s \quad (13)$$

and

$$\Upsilon^2(\theta) = \exp(-2A_1 m_v h \sec \theta), \quad (14)$$

where A_1 and C are constants for a given crop type and sensor configuration (wave-

length, polarization, and incidence angle), m_v and h are physical parameters of the vegetation canopy, and m_s is the soil moisture content. As was mentioned earlier, Attema and Ulaby (1978) assumed that the particles are all identical in size, which corresponds to the case where $f(N) = \text{const} = A_3$. By regressing experimental data against a model of the form given in (13), they determined the values of A_1 , A_3 , and C_s for several crops at each of several frequencies. In a more recent study, Hoekman et al. (1982) also found the cloud model to provide a good description of the temporal behavior of the backscattering coefficient for several crop types. For cereal grains, however, the model failed to predict the large changes in σ_{can}^0 that were observed in conjunction with the appearance of the wheat heads. This led Hoekman et al. (1982) to subdivide the vegetation layer into two sublayers: a lower layer representing the stalks and leaves and an upper layer representing the ears or heads. Using this two-layer form of the model, they obtained good agreement between measured and model-predicted values of σ_{can}^0 over the full growth cycle for each of eight crops.

Description of Experiment

In an effort to investigate further the connection between the physical parameters of the canopy (m_v , h , LAI, etc.) and the radar backscattering coefficient σ_{can}^0 , field experiments were conducted at a test site near Manhattan, Kansas, during the growing seasons of 1979 and 1980. The experiments were conducted by the Remote Sensing Laboratory of the University of Kansas in cooperation with the

TABLE 1 Experiment Data Summary^a

1979 EXPERIMENT			
CROP	No. OF FIELDS	START/STOP DATES	No. OF OBSERVATIONS PER FIELD
Wheat	2	4/26-7/2	10
Corn	6	6/5-9/11	6
Sorghum	6	6/5-9/11	6
1980 EXPERIMENT			
Corn	3	6/6-9/10	23
Sorghum	3	6/6-9/10	24

^aRadar parameters: angle of incidence θ : 50° (also 30° and 70° in 1979); polarization: VV, VH, HH; frequencies: 8.6, 13.0, 17.0, 35.6 GHz.

Evapotranspiration Laboratory at Kansas State University, Manhattan.

A truck-mounted scatterometer was used to measure σ_{can}^0 at 8.6, 13.0, 17.0, and 35.6 GHz (or equivalently, $\lambda = 3.5$ cm, 2.3 cm, 1.76 cm, and 8.4 mm). A total of 14 fields were observed in 1979, six each of corn and sorghum, and two of wheat (see Table 1). Each observation sequence consisted of measurements at angles of incidence θ of 30°, 50°, and 70° for each of three linear polarization configurations (HH, HV, VV). In 1980, the observations were limited to $\theta = 50^\circ$, and the number of fields was reduced to six, thereby increasing the number of temporal observations per field from an average of seven for 1979 to 23 for 1980.

In support of and contemporaneously with the radar observations, several plant and soil properties were measured, including plant height, the fresh weight W_w , and dry weight W_d of individual plant parts (leaves, stalks, and fruit), the LAI, soil moisture content m_s of the top 5-cm layer, planting density N_p (plants \cdot m⁻²), and stage of growth. The volumetric water content of the canopy can be

determined from

$$m_v = (W_w - W_d)N_p/h, \quad (15)$$

where W_w and W_d are the average wet and dry weights of an entire plant.

Examples of the observed temporal patterns of σ_{can}^0 are shown in Figs. 3-5 for winter wheat, corn, and sorghum, all at 13.0 GHz, $\theta = 50^\circ$, and VV polarization configuration. Also shown in these figures are plots of the green-leaf area index that show a fair degree of similarity to the plots of σ_{can}^0 , except for the period preceding harvest. It was also observed from the field data that the leaf area index (LAI) was highly correlated to the dry ($r^2 \cong 0.65$) and to the wet ($r^2 \cong 0.85$) (leaf) vegetation biomasses. This proves to be an important link, as will become apparent in the next section.

Due to space limitations, only samples of the measured data and the results of analysis are presented in this paper. Full documentation is available in a technical report (Ulaby et al., 1983).

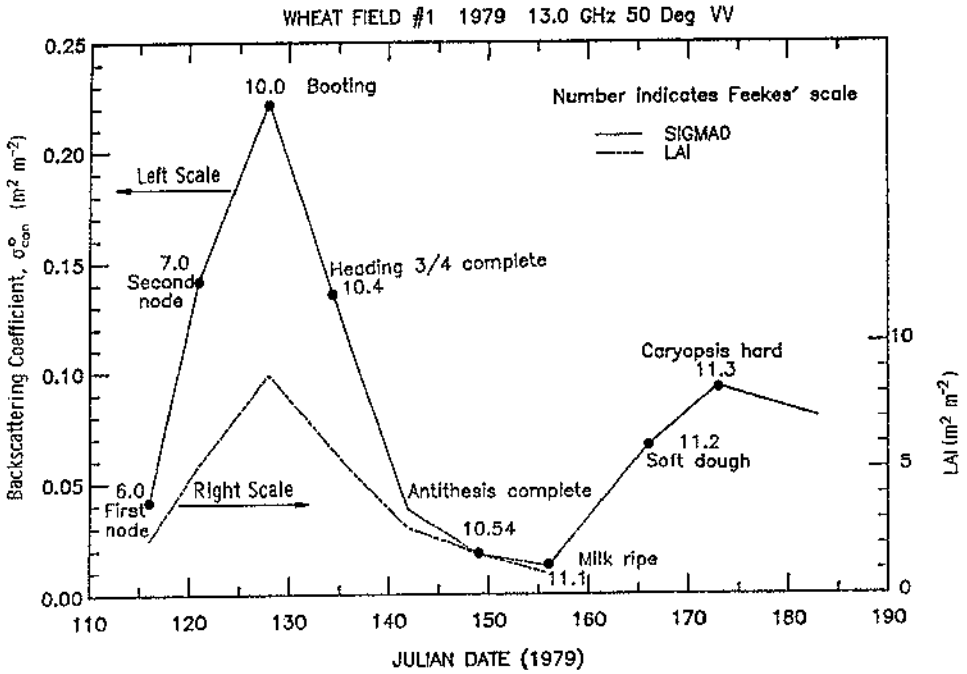


FIGURE 3. Measured temporal patterns of the backscattering coefficient and leaf-area index (LAI) of a wheat field. Stage of growth is indicated by the Feekes scale (Large, 1954).

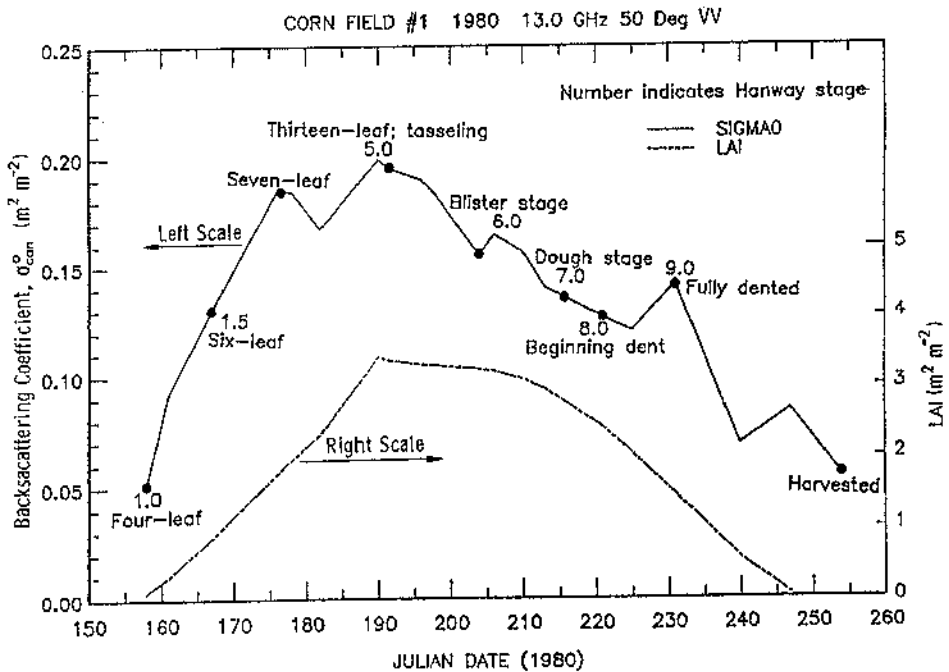


FIGURE 4. Measured temporal patterns of the backscattering coefficient and leaf-area index (LAI) of a corn field. Stage of growth is indicated by the Hanway stage (Hanway, 1971).

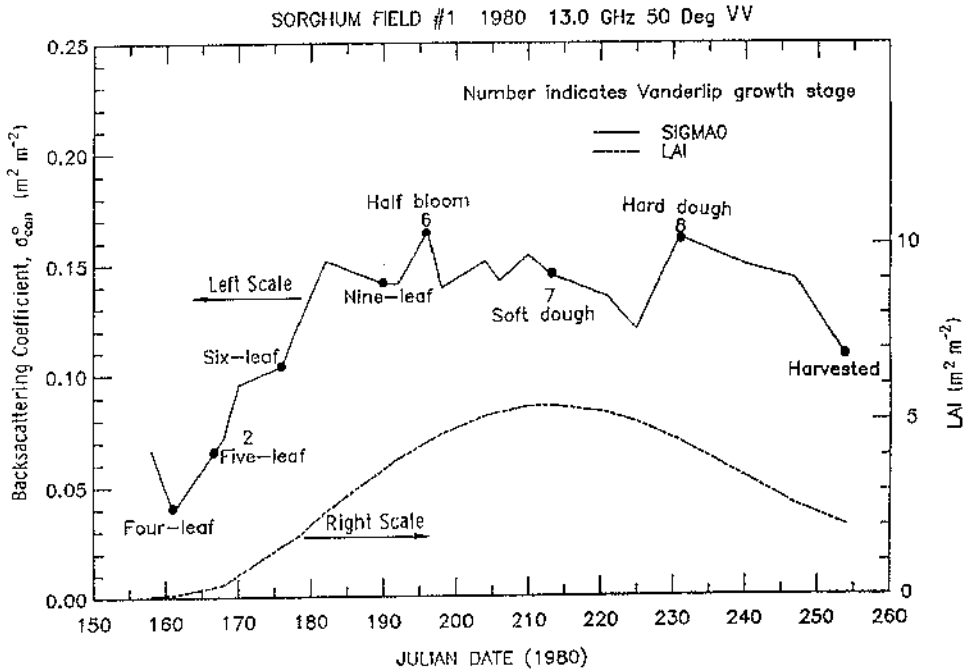


FIGURE 5. Measured temporal patterns of the backscattering coefficient and leaf-area index (LAI) of a sorghum field. Stage of growth is indicated by the Vanderlip growth stage (Vanderlip, 1972).

Multicomponent Cloud Model

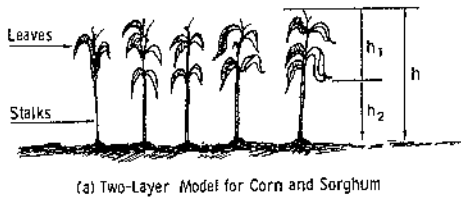
After completion of the processing and calibration of the data described in the previous section, the data were used to evaluate the applicability of the model given by (13). First, the model was evaluated by correlating the measured value of σ_{can}^0 to the value calculated using (13), with the constants A_1 , A_4 , and C_s being assigned the values that were determined by Attema and Ulaby (1978). This resulted in a multiple correlation coefficient r^2 between 0.4 and 0.7 (for the various combinations of crop type, microwave frequency, angle of incidence, and polarization). Next, another correlation analysis between measured and calculated values of σ_{can}^0 was performed, except that this time the constants were first determined empirically by regressing the data against the model. Some im-

provement in the magnitude of r^2 was obtained, but r^2 exceeded 0.7 only in a few cases.

To improve the applicability of the cloud model, two modifications were made, both of which resulted in better agreement between the measured temporal pattern of σ_{can}^0 and that calculated by the model.

Corn and sorghum

The first modification provides for separate accounting for the radar backscattering contributions of the leaves, the stalks, and the soil. For corn and sorghum, the canopy was assumed to consist of two layers: an upper layer of height h_1 , dominated by leaves, and a lower layer of height h_2 , dominated by stalks [Fig. 6(a)]. The backscattering contribution of the fruit was ignored, in part to simplify the



(a) Two-Layer Model for Corn and Sorghum



(b) Model for Wheat after Heading

FIGURE 6. Two-layer model for (a) corn and sorghum and (b) for wheat after heading.

model, and in part because of the results of a defoliation experiment for corn which showed that the backscattering contribution of the fruit is much smaller than that of the stalks or leaves (Ulaby, 1982). These assumptions lead to

$$\sigma_{can}^0(\theta) = \sigma_l^0(\theta) + \sigma_{st}^0(\theta) + \sigma_s^0(\theta), \quad (16)$$

where $\sigma_l^0(\theta)$ has the same form as (4),

$$\sigma_l^0(\theta) = \frac{\sigma_{vl} \cos \theta}{2\kappa_{el}} [1 - \Upsilon_l^2(\theta)], \quad (17)$$

and

$$\Upsilon_l^2(\theta) = \exp(-2\kappa_{el}h_1 \sec \theta). \quad (18)$$

In the above expressions, h_1 is the "effective" height of the top layer, assumed to consist of leaves exclusively, and σ_{vl} and κ_{el} are the volume backscattering coefficient and extinction coefficient of that layer. The stalk's contribution was

assumed to be given by

$$\sigma_{st}^0(\theta) = \Upsilon_l^2(\theta) \sigma_{st}^0(\theta; h_1 = 0), \quad (19)$$

where $\sigma_{st}^0(h_1 = 0)$ is the stalk contribution in the absence of leaves. Finally, the soil component is given by a form similar to that of (6) except that the attenuation through the canopy is now due to two layers: a top layer with transmission coefficient Υ_l and a lower layer with transmission coefficient Υ_{st} ,

$$\sigma_s^0(\theta) = [C_s(\theta)m_s] \Upsilon_l^2(\theta) \Upsilon_{st}^2(\theta), \quad (20)$$

where

$$\Upsilon_{st}^2(\theta) = \exp(-2\kappa_{es}h_2 \sec \theta) \quad (21)$$

and κ_{es} is the extinction coefficient of the stalk layer.

The second modification to the model involves the use of green LAI. Earlier, σ_{can}^0 was expressed in terms of three physical parameters: the soil moisture content m_s , the volumetric water content of the canopy m_v , and the canopy height h . Actually, the key quantity driving the model is the product $m_v h$, which represents the total amount of integrated water contained in a vertical column of unity horizontal cross section. The model in this section divides the canopy into two layers, with the top layer assumed to contain essentially all the leaves and the bottom layer assumed to contain the entire length of the stalk. The quantity $m_v h_1$ for the top layer is related to the wet and dry biomasses of the leaves, which in turn are related to the green LAI (Zrust et al., 1974; Ashley et al., 1965; Aase, 1978; Holben and Fan, 1980). Hence, instead of expressing Υ_l in terms of $m_v h_1$ [as in

(14)], it will be defined in terms of the leaf area index L ,

$$\Upsilon_l^2(\theta) = \exp(-2\alpha_l L \sec \theta). \quad (22)$$

For the stalk layer, it will be assumed that the scattering by the stalks, as well as the attenuation by them, is proportional to $m_v h_2$, where m_v is the volumetric water content of the stalk layer and h_2 is their effective height; hence,

$$\sigma_{st}^0(\theta) = A_{st} m_v h_2 \Upsilon_l^2(\theta) \sin \theta \quad (23)$$

and

$$\Upsilon_{st}^2(\theta) = \exp(-2\alpha_{st} m_v h_2 \sec \theta), \quad (24)$$

where A_{st} and α_{st} are constants (for a given crop type, microwave frequency, and polarization). Finally, it will be assumed that $f(N)$ of (12) is given by

$$f(N) = A_l [1 - \exp(-B_l L/h_1)], \quad (25)$$

where A_l and B_l are constants for a given crop type at a given frequency, angle, and polarization configuration. In general, $f(N)$ is proportional to the scattering albedo of the leaf layer of the canopy. For low values of the number density of scatterers N , the albedo increases in an approximately linear fashion with N . For N large, the albedo reaches a saturation level. This behavior can be described by the functional form given by (25), with L/h_1 , the leaf area index divided by the height of the leaf layer, serving as a measure of number density of scatterers.

Grouping the above term leads to

$$\begin{aligned} \sigma_{can}^0(\theta) = & A_l [1 - \exp(-B_l L/h_1)] \\ & \times \cos \theta [1 - \Upsilon_l^2(\theta)] \\ & + A_{st} m_v h_2 \Upsilon_l^2(\theta) \sin \theta \\ & + [C_s(\theta) m_s] \Upsilon_l^2(\theta) \Upsilon_{st}^2(\theta). \end{aligned} \quad (26)$$

The above expression contains six coefficients and four physical parameters: (a) green LAI, (b) effective height of the leaf layer h_1 , (c) $m_v h_2$, the total water content of the stalks per unit area, and (d) m_s , the volumetric soil moisture content. Because h_1 was not measured directly, it was assumed that h_1 is proportional to the total plant height h and h_1 was replaced with h in (26). The coefficients were determined by using a nonlinear regression program that minimizes the least-squares error between the predicted and observed values. Data from all three fields (of 1980 sorghum or 1980 corn) were used to generate the coefficients, and then the model was used to predict the temporal pattern of σ^0 for each field individually. The values of the coefficients obtained are given in Tables 2 and 3 for corn and sorghum, respectively. Also given is the correlation coefficient between the measured and predicted values of σ_{can}^0 for each field at each of the four frequencies. Figures 7 and 8 show comparisons for corn and sorghum, respectively. Each figure contains a plot of the predicted σ_{can}^0 , denoted σ_{pred}^0 , as well as plots of its component contributions as defined by (16). It is observed that:

- (a) Except for the period prior to Julian day 170 (for which the plant height

TABLE 2 Coefficients for the Corn Model Given by Eq. (26) Rewritten in the Abbreviated Form for $\theta = 50^\circ$ and VV Polarization^a

FREQUENCY (GHz)	A_l	B_l	α_l	A_{st} ($m^2 \cdot kg^{-1}$)	α_{st} ($m^2 \cdot kg^{-1}$)	C_s ($cm^3 \cdot g^{-1}$)	r^2 /RMS DIFF. ERROR (dB)/(N)			
							ALL FIELDS	FIELD 1	FIELD 2	FIELD 3
8.6	0.218	2.56	0.411	0.025	0	0.197	0.78 0.8/(69)	0.81 0.7/(21)	0.91 0.8/(22)	0.83 0.9/(26)
13.0	0.269	2.77	0.444	0.029	0	0.185	0.80 0.9/(69)	0.91 0.6/(21)	0.77 1.1/(22)	0.87 0.8/(26)
17.0	0.297	2.70	0.418	0.022	0	0.234	0.77 1.0/(69)	0.82 0.8/(21)	0.74 1.1/(22)	0.92 0.9/(26)
35.0	0.359	2.01	0.360	0.034	0	0.133	0.87 0.8/(65)	0.91 0.7/(20)	0.81 1.0/(20)	0.91 0.8/(25)

a

$$\begin{aligned}\sigma_{can}^0 &= \sigma_l^0 + \alpha_{st}^0 + \sigma_s^0 \\ &= A_l [1 - \exp(-B_l \cdot L/h)] [1 - T_l^2] \cos \theta \\ &\quad + A_{st} \cdot m_v \cdot h_2 \cdot T_l^2 \\ &\quad + C_s \cdot m_s \cdot T_l^2 \cdot T_{st}^2,\end{aligned}$$

where

$$T_l^2 = \exp(-2\alpha_l \cdot \sec \theta \cdot L)$$

$$T_{st}^2 = \exp(-\alpha_{st} \cdot m_v \cdot h_2)$$

and $h_2 = h$, the canopy height. The coefficients were determined through the use of a nonlinear regression program. The correlation coefficient r^2 is the linear correlation between the observed values σ_{obs}^0 and the predicted values σ_{pred}^0 . The RMS difference error (dB) is determined by the following equation:

$$\text{RMS Diff. Error (dB)} = \left[\frac{\sum_{i=1}^N (\sigma_{obs}^0(\text{dB})_i - \sigma_{pred}^0(\text{dB})_i)^2}{N} \right]^{1/2}$$

was less than 0.8 m for corn and less than 0.6 m for sorghum) and for the preharvest period after Julian day 240, the leaves provide the overwhelming majority of the backscattered energy.

- The soil and stalk terms are important only if LAI < 0.5.
- A better fit could be obtained for corn if the leaf attenuation coefficients α_l were to be assigned different values for the two periods before and after Julian day 190, which corresponds to the date at

which the LAI reaches its peak value. It has been suggested that the optical transmission properties of leaves change in magnitude as the plant enters the senescence phase. The same may be true for the microwave part of the spectrum, but no data exist at present to support such a hypothesis.

Wheat

Wheat has a significantly different geometry than that of corn or sorghum,

TABLE 3 Coefficients for the Sorghum Model Given by Eq. (26) Rewritten in Abbreviated Form for $\theta = 50^\circ$ and VV Polarization^a

FREQUENCY (GHz)	A_l	B_l	α_l	A_{st} ($m^2 \cdot kg^{-1}$)	α_{st} ($m^2 \cdot kg^{-1}$)	C_s ($cm^2 \cdot g^{-1}$)	r^2 /RMS Diff. Error (dB)/(N)			
							ALL FIELDS	FIELD 1	FIELD 2	FIELD 3
8.6	0.184	1.08	0.569	0.299	0	0.194	0.81	0.92	0.87	0.76
							0.7/(71)	0.4/(21)	0.6/(23)	0.9/(27)
13.0	0.235	1.00	0.569	0.318	0	0.212	0.87	0.88	0.72	0.89
							0.6/(71)	0.5/(21)	0.5/(23)	0.7/(27)
17.0	0.255	1.00	0.444	0.288	0	0.189	0.89	0.89	0.89	0.81
							0.6/(71)	0.6/(21)	0.7/(23)	0.6/(27)
35.6	0.263	24.4	0.466	0.6345	0	0.0772	0.87	0.86	0.93	0.89
							0.8/(67)	0.9/(20)	0.7/(21)	0.7/(26)

^a

$$\begin{aligned} \sigma_{can}^0 &= \sigma_l^0 + \alpha_{st}^0 + \alpha_s^0 \\ &= A_l [1 - \exp(-B_l \cdot L/h)] [1 - T_l^2] \cos \theta \\ &\quad + A_{st} \cdot m_o \cdot h_2 \cdot T_l^2 \\ &\quad + C_s \cdot m_s \cdot T_l^2 \cdot T_{st}^2 \end{aligned}$$

where

$$T_l^2 = \exp(-2\alpha_l \cdot \sec \theta \cdot L)$$

$$T_{st}^2 = \exp(-\alpha_{st} \cdot m_o \cdot h_2),$$

and $h_2 = h$, the canopy height. The coefficients were determined through the use of a nonlinear regression program. The correlation coefficient r^2 is the linear correlation between the observed values σ_{obs}^0 and the predicted values σ_{pred}^0 . The RMS Difference Error (dB) is determined by the following equation:

$$\text{RMS diff. error (dB)} = \left[\frac{\sum_{i=1}^N (\sigma_{obs}^0(\text{dB}) - \sigma_{pred}^0(\text{dB}))^2}{N} \right]^{1/2}$$

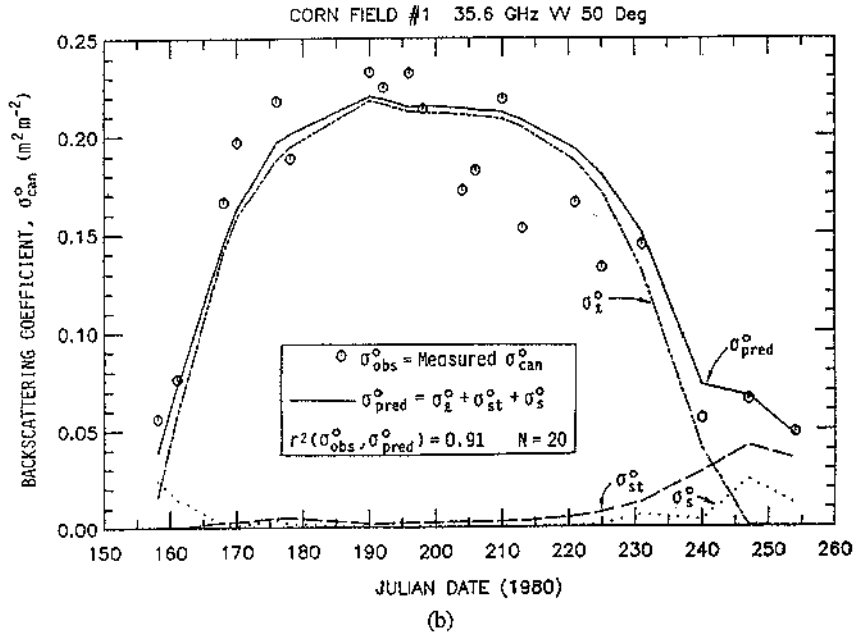
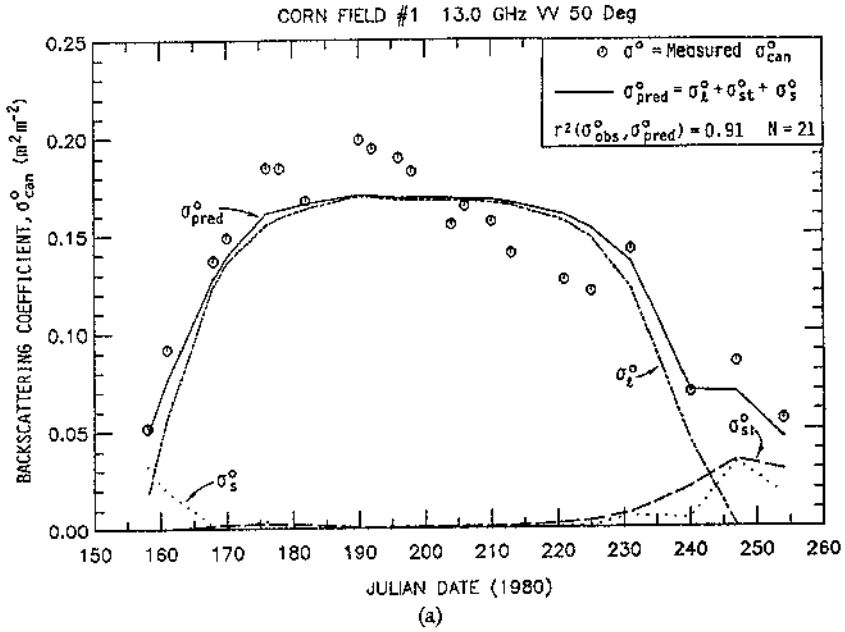


FIGURE 7. Comparison of measured backscattering coefficient of corn with that computed using Eq. (25) at (a) 13.0 GHz and (b) 35.6 GHz, 50° incidence angle, and VV polarization.

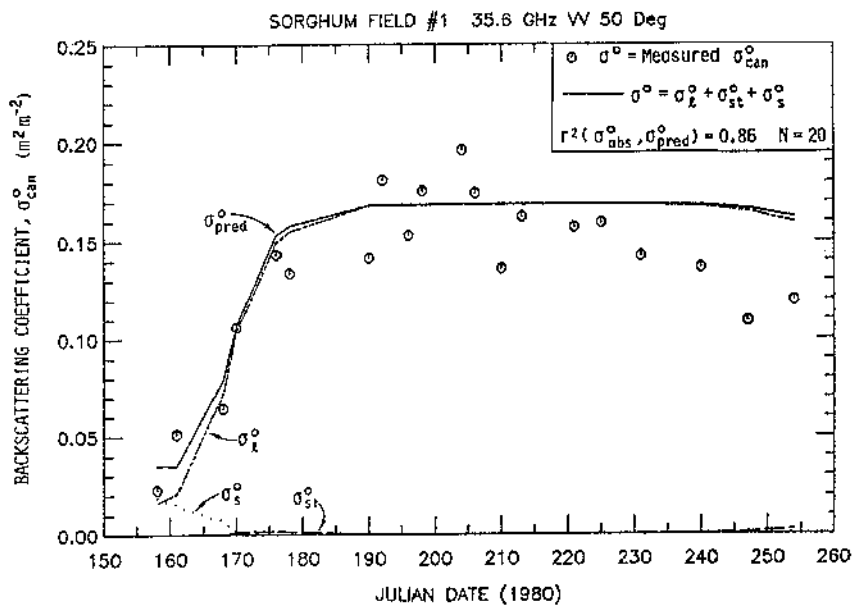
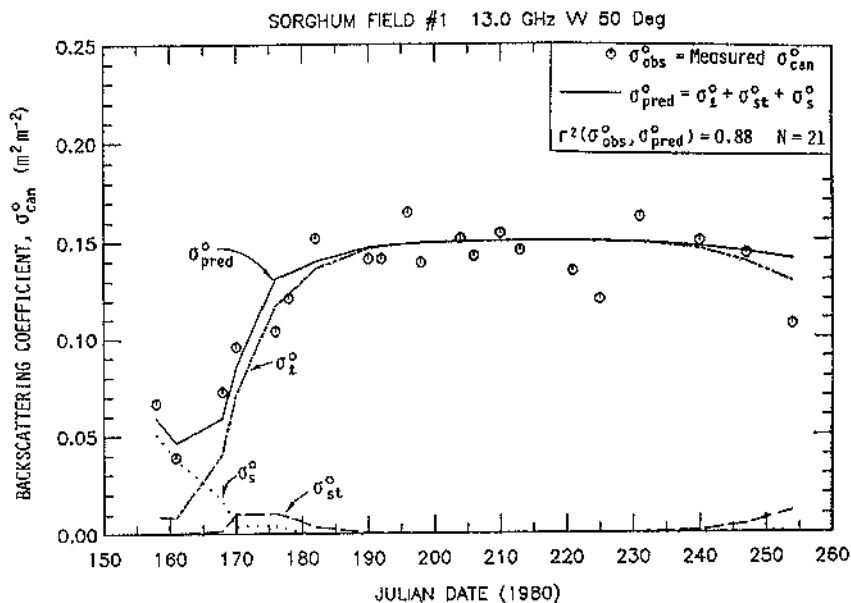


FIGURE 8. Comparison of measured backscattering coefficient of sorghum with that computed using Eq. (25) at (a) 13.0 GHz and (b) 35.6 GHz, 50° incidence angle, and VV polarization.

thereby necessitating that certain modifications be introduced to the model described in the previous section. First, the wheat stalks are much smaller and contain a smaller portion of the total plant water. Hence, the stalk's backscattering contribution will be neglected. Secondly, the size, location, and relative water content of the heads suggest that their backscattering contributions should be accounted for explicitly (rather than being ignored or lumped with the stalks, as was done in the previous section for corn and sorghum). Additionally, since the heads of the wheat plants are above the leaves [Fig. 6(b)], the leaves should not attenuate the backscattering from the head; rather, it should be the other way around. These modifications, plus some others discussed below, lead to the expression

$$\begin{aligned}\sigma_{\text{can}}^0(\theta) &= \sigma_l^0(\theta) + \sigma_h^0(\theta) + \sigma_s^0(\theta) \\ &= A_l [1 - \exp(-B_l L/h)] \\ &\quad \times [1 - \Upsilon_l^2(\theta)] \Upsilon_h^2 \cos \theta \\ &\quad + A_h(\theta) \cdot M_h \\ &\quad + C_s(\theta) m_s \Upsilon_l^2(\theta) \Upsilon_h^2(\theta),\end{aligned}\quad (27)$$

where $\Upsilon_l^2(\theta)$ is given by (22), M_h is the head biomass ($\text{kg} \cdot \text{m}^{-2}$), h is the height of the canopy, and

$$\Upsilon_h^2(\theta) = \exp(-2\alpha_h M_h \sec \theta). \quad (28)$$

The field measurements did not include direct measurements of the head's biomass M_h ; therefore, an estimate was needed. If the plant is assumed to be fully developed before heading takes place, then the dry weight due to the leaves and stalks should remain constant for the

period during and after heading (assuming no leaves fall off the plant). Any change in dry weight after the onset of heading will therefore be directly related to the development of the head. This reasoning leads to

$$M_h(t) = \begin{cases} 0, & \text{for } t < t_0 \\ W_d(t) - W_d(t_0), & \text{for } t > t_0, \end{cases} \quad t_0 = \text{heading date}$$

where W_d is the total plant dry biomass ($\text{kg} \cdot \text{m}^{-2}$). For the fields observed in 1979, $t_0 = 136$ (16 May 1979).

Following a determination of the values of the six coefficients employed in the model (see Table 4), plots were generated to compare σ_{pred}^0 to σ_{obs}^0 . Examples are shown in Figs. 9(a) and 9(b) for 13 GHz and 35.6 GHz, respectively. In both cases, the model provides a good fit to the measured data, and indicates that the backscattering is almost exclusively due to the leaves for the period between Julian days 120 and 155. After Julian day 155, green LAI goes to zero, and the observed backscattering becomes due entirely to the heads and the soil surface.

Approximate Form in Terms of LAI

The models discussed in the previous section appear to agree well with experimental observations, which makes them useful tools for evaluating the sensitivity of the radar backscattering coefficient to the physical parameters of the plant canopy and soil surface. From an applications standpoint, however, radar would be far more useful if the backscattering coefficient it measures could be used to estimate a single, but important, physical

TABLE 4 Coefficients for the Wheat Model Given by Eq. (27), Rewritten in the Following Abbreviated Form for $\theta = 50^\circ$ and VV Polarization^a

FREQUENCY (GHz)	A_l	B_l	α_l	A_h ($m^2 \cdot kg^{-1}$)	α_h ($m^2 \cdot kg^{-1}$)	C_s	r^2 /RMS DIFF. ERROR (dB)/(N)		
							ALL FIELDS	FIELD 1	FIELD 2
8.6	2.02	0.0075	0.829	0.116	2.15	0.488	0.57 1.6/(20)	0.68 1.7/(10)	0.49 1.6/(10)
13.0	6.57	0.0032	2.75	0.0415	2.57	0.629	0.77 1.6/(18)	0.86 1.4/(10)	0.62 1.9/(18)
17.0	15.1	0.0018	1.03	0.0317	1.14	0.533	0.86 1.3/(19)	0.90 1.3/(10)	0.82 1.3/(9)
35.6	28.3	0.0007	8.65	0.028	2.45	0.292	0.80 1.7/(20)	0.89 1.4/(10)	0.70 2.0/(10)

^a

$$\begin{aligned}\sigma_{can}^0 &= \sigma_l^0 + \sigma_h^0 + \sigma_s^0 \\ &= A_l [1 - \exp(-B_l \cdot L/h)] [1 - T_l^2] T_h^2 \cos \theta \\ &\quad + A_h \cdot M_h \\ &\quad + C_s \cdot m_s \cdot T_l^2 \cdot T_h^2\end{aligned}$$

where $T_l^2 = \exp(-2\alpha_l \cdot \sec \theta \cdot L)$. The coefficients were determined through the use of a nonlinear regression program. The correlation coefficient r^2 defines the linear correlation between the observed values σ_{obs}^0 and the predicted values σ_{pred}^0 . The RMS difference error in (dB) is determined by the following equation:

$$\text{RMS diff. error (dB)} = \left[\frac{\sum_{i=1}^N (\sigma_{obs}^0(\text{dB})_i - \sigma_{pred}^0(\text{dB})_i)^2}{N} \right]^{1/2}$$

parameter of the canopy, such as green LAI. The conclusions arrived at in the previous section relevant to the temporal "signature" of σ_{can}^0 may be summarized as follows:

(a) During the early stage of growth (short plants and $LAI < 0.5$), the magnitude of σ_{can}^0 may be affected, even dominated, by soil-moisture conditions.

(b) During the stage of growth characterized by $LAI > 0.5$, σ_{can}^0 is dominated by the leaf contributions. Hence, $\sigma_{can}^0 \cong \sigma_l^0$ for $LAI \geq 0.5$.

(c) During the stage of growth prior to harvest and $LAI < 0.5$, σ_{can}^0 is dominated by the soil and stalk contributions for corn and sorghum and by the soil and head contributions for wheat.

Based on the above observations, let us examine the behavior of σ_{can}^0 as a function of LAI alone. To reduce the effects of soil moisture variations we shall limit the examination to data for which $LAI \geq 0.2$. Figures 10 to 12 present data measured at 13 GHz for all fields of corn, sorghum, and wheat, respectively, plotted as a function of LAI for $LAI \geq 0.2$. The data can be fitted to empirical functions of the form:

$$\begin{aligned}\sigma_{can}^0(L) &= A'_l L^n [1 - \exp(-\alpha'_l L)] \\ &\quad + C'_s \exp(-\alpha'_l L)\end{aligned}\quad (29)$$

where A'_l , α'_l , and C'_s are constants, and $n = 0$ for corn and sorghum and 1 for

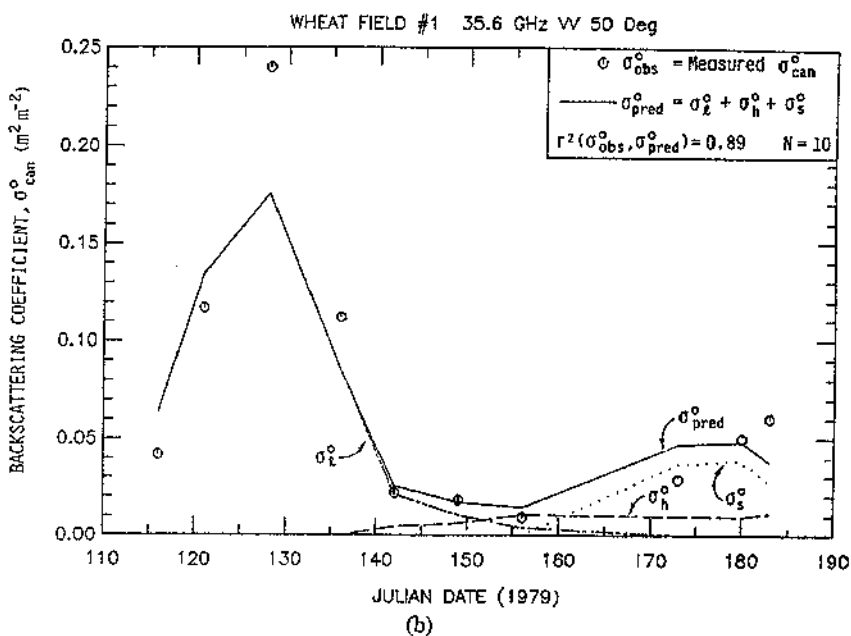
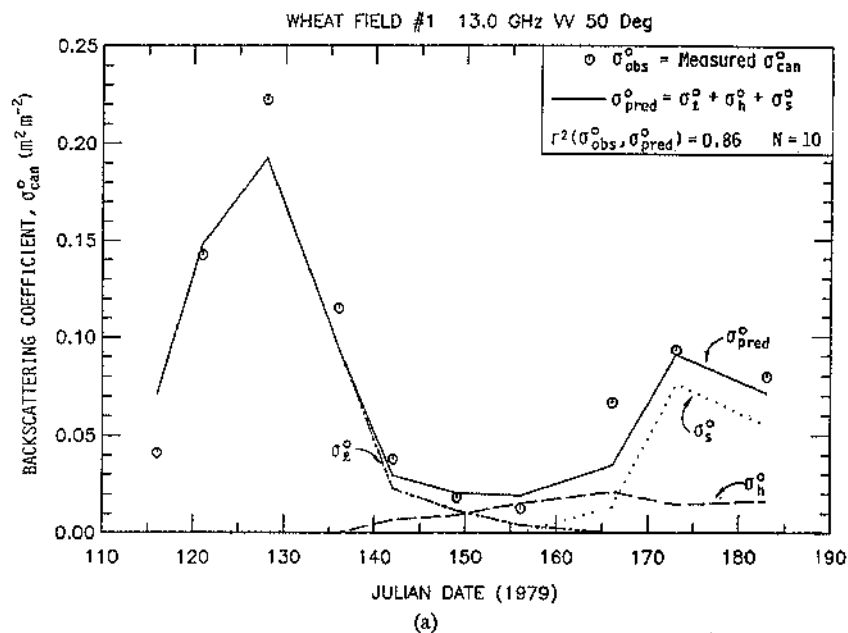


FIGURE 9. Comparison of measured backscattering coefficient of wheat with that computed using Eq. (26) at (a) 13.0 GHz and (b) 35.6 GHz, 50° incidence angle, and VV polarization.

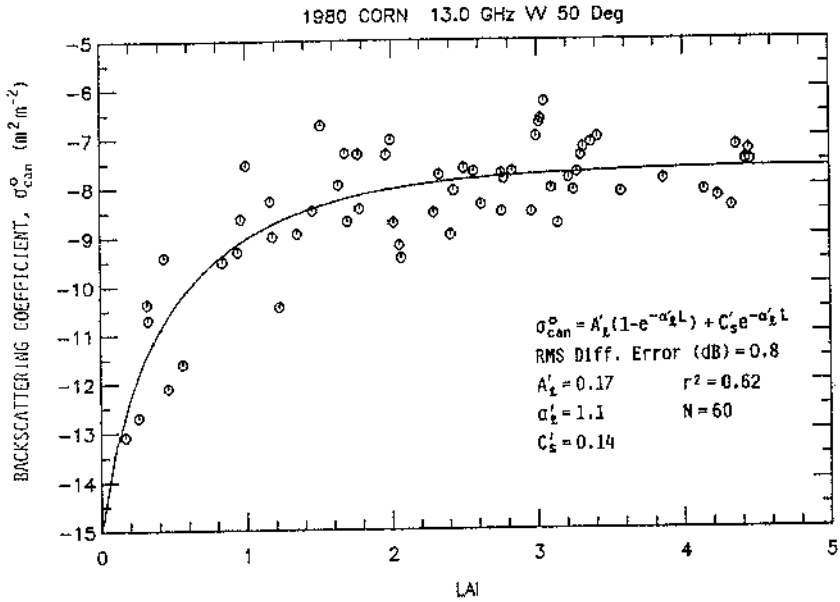


FIGURE 10. Comparison of measured backscattering coefficient of corn with that computed on the basis of the single-parameter (LAI) model.

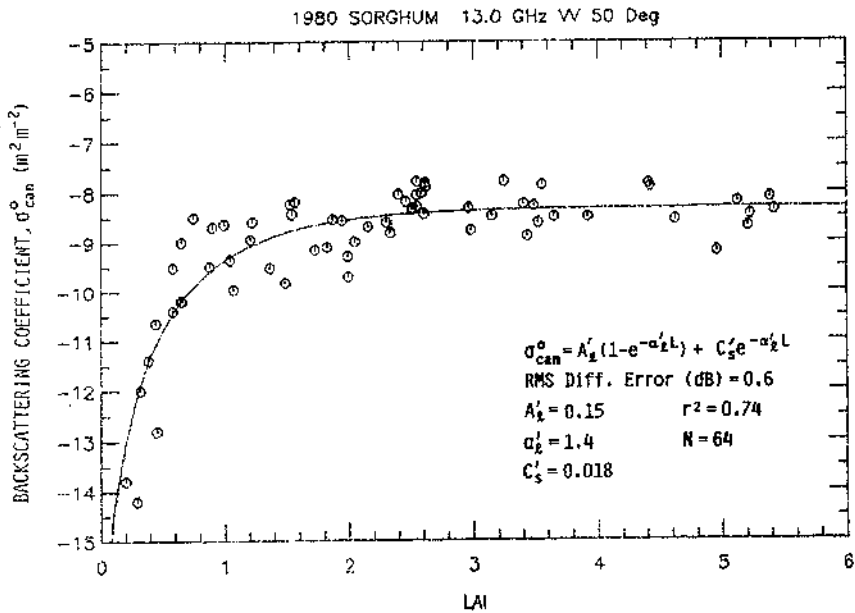


FIGURE 11. Comparison of measured backscattering coefficient of sorghum with that computed on the basis of the single-parameter (LAI) model.

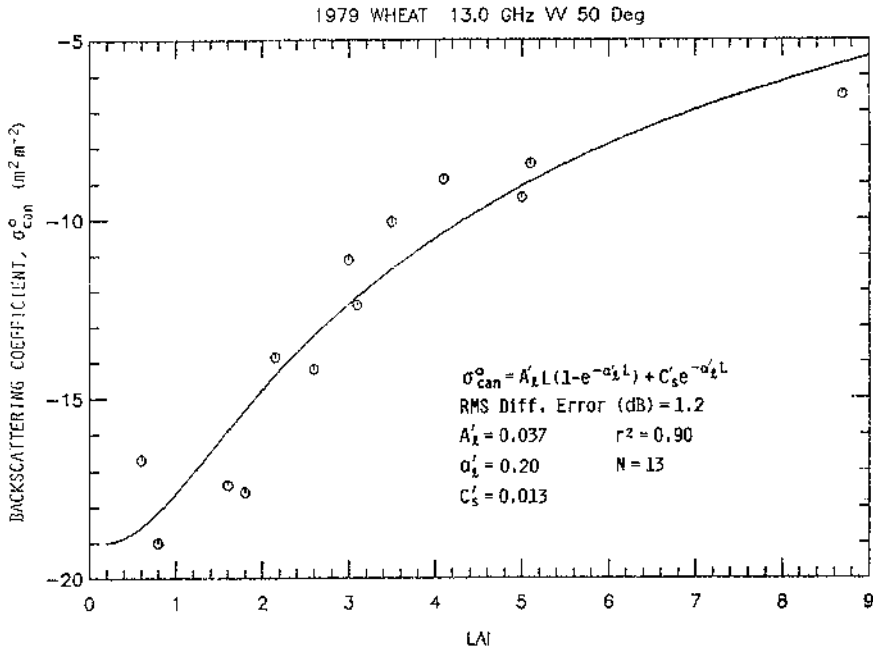


FIGURE 12. Comparison of measured backscattering coefficient of wheat with that computed on the basis of the single-parameter (LAI) model.

wheat. The results show that for corn and sorghum, σ_{can}^0 increases with increasing LAI up to $L \cong 2$. Beyond this value, the sensitivity $d\sigma_{\text{can}}^0/dL \cong 0$. In contrast, wheat shows a weaker sensitivity to L , but σ_{can}^0 remains sensitive to L over a much wider dynamic range. The data scatter observed in Figs. 10–12 is due to several sources, including (a) sensor measurement precision, estimated to be about ± 1 dB, (b) soil moisture variations, (c) errors associated with the measurement of LAI, and (d) within-field and between-field variations that are not accounted for by the model or the data.

Conclusions

By extending the canopy cloud model of Attema and Ulaby (1978) from its initial consideration of the canopy as a single layer with uniform volume scattering and

attenuation properties to one consisting of more than one layer, it was possible to examine the relative backscattering contributions of the leaves, stalks, and heads (of wheat). The analysis of radar backscattering data measured at an incidence angle of 50° and microwave frequencies of 8.6, 13.0, 17.0, and 35.6 GHz indicates that the backscattering coefficient of the canopy is dominated by the leaf contribution if green LAI is greater than approximately 0.5 for corn and sorghum and if, additionally, the heads have not yet appeared (for wheat). During the early stage of growth, a soil backscattering contribution may be very important, and for the end-period prior to harvest, the backscattering contributions of the soil and the stalks are important for sorghum and corn, and of the heads and soil for wheat. A simplified version of the model was developed in terms of a single parameter, green LAI.

This research was supported by the National Aeronautics and Space Administration, Lyndon B. Johnson Space Center, Houston, Texas, under Contract NAS 9-15421.

References

- Aase, J. K. (1978), Relationship between leaf area and dry matter in winter wheat, *Agron. J.* 70:563-565.
- Ashley, D. A., Doss, B. D., and Bennett, O. L. (1965), Relation of cotton leaf area index to plant growth and fruiting, *Agron. J.* 57:61-64.
- Attema, E. P. W., and Ulaby, F. T. (1978), Vegetation modeled as a water cloud, *Radio Sci.* 13(2):357-364.
- Brisco, B., and Protz, R. (1980), Corn field identification accuracy using airborne radar imagery, *Can. J. Remote Sens.* 6(1):15-25.
- Bush, T. F., and Ulaby, F. T. (1978), An evaluation of radar as a crop classifier, *Remote Sens. Environ.* 7:15-36.
- Carlson, N. L. (1967), Dielectric constant of vegetation at 8.5 GHz, Ohio State University ElectroScience Laboratory Technical Report 1903-5, Columbus, Ohio.
- Coelho, D. T., and Dale, R. F. (1980), An energy-crop growth variable and temperature function for predicting corn growth and development: Planting to silking, *Agron. J.* 72:503-510.
- Dale, R. F. (1977), An energy-crop growth variable for identifying weather effects upon maize yields, in *Agrometeorology of Maize (Corn) Crop* (W. Baier, R. H. Shaw, L. M. Thomson, and R. E. Felch, eds.), *Proceedings of the Symposium on Agrometeorological Maize (Corn) Crop*, World Meteorological Organization, Iowa State University, Ames, Iowa, 5-9, July 1976, WMO No. 481, Geneva, Switzerland.
- Daughtry, C. S. T., and Fuhs, N. C. (1980), Determination of the value of spectral information in estimation of agronomic variables associated with yields of corn and soybeans, *AgRISTARS Report SR-P0-04023*, pp. 33-54.
- Daughtry, C. S. T., Gallo, K. P., and Bauer, M. E. (1983), Spectral estimates of solar radiation intercepted by corn canopies, *Agron. J.* 75:527-531.
- Hanway, J. J. (1971), How a corn plant develops. Special Report No. 48, Iowa State University, Cooperative Extension Service, Ames, Iowa.
- Hoekman, D. H., Krul, L., and Attema, E. P. W. (1982), A multilayer model for radar backscattering from vegetation canopies, *Digest, Second Annual International Geoscience and Remote Sensing Symposium*, Vol. II, Munich, West Germany, 1-4 June (IEEE Catalogue No. 82CH14723-6).
- Holben, B. N., and Fan, C. (1980), Spectral assessment of soybean leaf area and leaf biomass, *Photogramm. Eng. Remote Sens.* 46(5):651-656.
- Hoogeboom, P. (1982), Classification of agricultural crops in radar images, *Digest, Second Annual International Geoscience and Remote Sensing Symposium*, Vol. II, Munich, West Germany, 1-4 June (IEEE Catalogue No. 82CH14723-6).
- Jedlicka, R. P., and Ulaby, F. T. (1983), Measurements of the radar microwave dielectric and attenuation properties of plants. Proceedings of the National Radio Science Meeting (URSI Commission F), 5-7 January, University of Colorado, Boulder, Colorado.
- Large, E. C. (1954), Growth stages in cereals, illustration of the Feekes scale, *Plant Pathol.* 3:128-129.
- Li, R. Y., Ulaby, F. T., and Eyton, J. R. (1980), Crop classification with a Landsat/Radar sensor combination, presented at the Sixth Purdue Symposium on Machine Processing of Remotely Sensed Data, 2-6 June, Purdue University, West Lafayette,

- Indiana, supported by NASA Contract NAS 9-15421.
- Linville, D. E., Dale, R. F., and Hodges, H. F. (1978), Solar radiation weighting for weather and corn growth models, *Agron. J.* 70:257-263.
- MacDonald, R. B., and Hall, F. G. (1980), Global crop forecasting, *Science* 208:670-679.
- Shanmugan, K. S., Ulaby, F. T., Narayanan, V., and Dobson, M. C. (1983), Identification of corn fields using multirate radar data, *Remote Sens. Environ.* 13:251-264.
- Stuff, R. B., and Dale, R. F. (1978), A soil moisture budget model for accounting for shallow water table influences, *Soil. Sci. Soc. Am. J.* 42:637-643.
- Tucker, C. J., Holben, B. N., Elgin, J. H., Jr., and McMurtrey, J. E., III (1981), Remote sensing of total dry matter accumulating in winter wheat, *Remote Sens. Environ.* 11:171-189.
- Ulaby, F. T. (1982), Review of approaches to the investigation of the scattering properties of material media, *Digest Second Annual International Geoscience and Remote Sensing Symposium*, Munich, West Germany, 1-4 June (IEEE Catalogue No. 82CH14723-6).
- Ulaby, F. T., Allen, C., Eger, G., III, and Kanemasu, E. (1983), Relating the radar backscattering coefficient to leaf-area index, RSL Technical Report 460-16, University of Kansas Center for Research, Inc., Lawrence, Kansas.
- Vanderlip, R. L. (1972), How a sorghum plant develops, Contribution No. 1203, Agronomy Department, Kansas Agricultural Experiment Station, Manhattan, Kansas.
- Zadoks, J. C., Chang, T. T., and Konzak, C. F. (1974), A decimal code for the growth stages of cereals, *Weed Res.* 14:415-421.
- Zrust, J., Partykova, E., and Necas, J. (1974), Relationship of leaf area to leaf weight and length in potato plants, *Photosynthetica (Prague)* 8:118-124.

Received 30 March 1983; revised 19 September 1983.